

Mapping Disease Course Across the Mood Disorder Spectrum Through a Research Domain Criteria Framework

Alexis E. Whitton, Poornima Kumar, Michael T. Treadway, Ashleigh V. Rutherford, Manon L. Ironside, Dan Foti, Garrett Fitzmaurice, Fei Du, and Diego A. Pizzagalli

ABSTRACT

BACKGROUND: The National Institute of Mental Health Research Domain Criteria (RDoC) initiative aims to establish a neurobiologically valid framework for classifying mental illness. Here, we examined whether the RDoC construct of reward learning and three aspects of its underlying neurocircuitry predicted symptom trajectories in individuals with mood pathology.

METHODS: Aligning with the RDoC approach, we recruited individuals ($n = 80$ with mood disorders [58 unipolar and 22 bipolar] and $n = 32$ control subjects; 63.4% female) based on their performance on a laboratory-based reward learning task rather than clinical diagnosis. We then assessed 1) anterior cingulate cortex prediction errors using electroencephalography, 2) striatal reward prediction errors using functional magnetic resonance imaging, and 3) medial prefrontal cortex glutamatergic function (mPFC Gln/Glu) using ^1H magnetic resonance spectroscopy. Severity of anhedonia, (hypo)mania, and impulsivity were measured at baseline, 3 months, and 6 months.

RESULTS: Greater homogeneity in aspects of brain function (mPFC Gln/Glu) was observed when individuals were classified according to reward learning ability rather than diagnosis. Furthermore, mPFC Gln/Glu levels predicted more severe (hypo)manic symptoms cross-sectionally, predicted worsening (hypo)manic symptoms longitudinally, and explained greater variance in future (hypo)manic symptoms than diagnostic information. However, rather than being transdiagnostic, this effect was specific to individuals with bipolar disorder. Prediction error indices were unrelated to symptom severity.

CONCLUSIONS: Although findings are preliminary and require replication, they suggest that heightened mPFC Gln/Glu warrants further consideration as a predictor of future (hypo)mania. Importantly, this work highlights the value of an RDoC approach that works in tandem with, rather than independent of, traditional diagnostic frameworks.

<https://doi.org/10.1016/j.bpsc.2021.01.004>

The Diagnostic and Statistical Manual of Mental Disorders (DSM) (1) and International Classification of Diseases (2) classify major depressive disorder (MDD) and bipolar disorder (BD) as separate conditions distinguishable by a history of (hypo)mania, with evidence supporting a disease-specific treatment approach (3,4). Although these nosological systems provide a useful common language for clinicians and researchers, their value for understanding mood disorder pathophysiology remains limited. Accordingly, the Research Domain Criteria (RDoC) (5,6) was proposed as a strategic change in scientific inquiry and seeks to classify psychiatric disorders according to measurable variability within and across different domains of functioning. Subsequently, the Positive Valence Systems domain—in particular, the subdomain of reward learning—has emerged as an especially promising target for understanding the mechanisms underpinning mood symptoms.

Reward learning refers to the ability to adaptively modulate behavior as a function of positive reinforcement. Abnormalities in reward learning and underlying neurocircuitry have been

strongly implicated in mood disorders (7,8). For example, performance on behavioral reward learning paradigms has been shown to 1) differentiate patients with MDD or BD from control subjects during symptomatic and asymptomatic states (9,10), 2) predict anhedonia severity and treatment outcome (11), 3) change following pharmacological dopaminergic manipulations (12,13), 4) be linked to striatal dopamine transporter function and frontostriatal functional connectivity (14), and 5) be heritable (15). Decades of research in laboratory animals has identified the neurobiological processes underpinning reward learning (16). Therefore, examining how these processes vary across the mood disorder spectrum represents a fruitful avenue for identifying the neurobiological basis underpinning mood disorder heterogeneity.

Imaging and computational studies suggest that the brain employs distinct hierarchical systems to support learning (17,18), and to date the neural circuitry involved in learning from positive reinforcement has been especially well characterized (19–21). Importantly, individuals with MDD or BD have

been found to exhibit dysregulation in three key aspects of this neurocircuitry. First, a fundamental mechanism that supports reward learning is the reward prediction error (RPE), which is a striatal dopamine-based signal that encodes violations of reward expectancies (22). Individuals with MDD have been found to have blunted striatal RPE signals during learning (23–25), and this blunting has been linked to a more recurrent depressive illness course (23). Similar abnormalities have been observed in individuals with BD, although the direction of effects often diverges from those observed in studies of unipolar MDD. Relative to healthy control subjects, euthymic individuals with BD or individuals with subthreshold hypomania have been found to have elevated striatal activation during reward anticipation (26) and reward outcome (27). Similarly, manic individuals with BD show striatal responses that fail to differentiate between receipt and omission of rewards, suggestive of abnormal RPE signaling (28).

Second, event-related potential (ERP) studies highlight the reward positivity (RewP) as another important reward circuit component linked to mood pathology (29). The RewP is a frontocentral electroencephalographic (EEG) deflection that is elicited by RPEs and is thought to originate from the anterior cingulate cortex (ACC) and striatum (30). Smaller RewP amplitudes, as well as weaker RewP-related ACC activation, predict poorer reward learning (31,32). Furthermore, abnormal RewP amplitudes have been observed in individuals with hypomania (33) and those with MDD (34), and they have been found to predict future depression onset in healthy individuals (35). Critically, the source of these RewP signals is believed to be distinct from that of striatal dopaminergic RPEs (36); hence, they offer complementary information to functional magnetic resonance imaging (fMRI)-based RPE studies in terms of understanding the biological basis of reward learning dysfunction.

Finally, while the reward learning literature has historically emphasized the role of dopamine, the hedonic effects of dopamine are thought to be partially mediated by its interactions with glutamatergic signals originating in the medial prefrontal cortex (mPFC) (37). In line with this notion, in animal studies disrupted glutamate signaling between mPFC and striatal regions impairs reward motivation (38), and in psychiatrically healthy humans mPFC glutamate levels (measured using magnetic resonance spectroscopy [MRS]) predict reward-based decision making (39). Human MRS studies often focus on the glutamine/glutamate ratio (Gln/Glu) because glutamate is released into the synaptic cleft, taken up by glial cells, converted into glutamine, and cycled back into neurons (40), making mPFC Gln/Glu a proxy measure of the integrity of the glutamatergic synapse. Of note, meta-analyses of MRS studies have highlighted mPFC glutamate abnormalities in MDD and BD, albeit in opposite directions, with glutamatergic transmission being reduced in MDD (41) but elevated in BD (42) across manic (43), depressive (44), and euthymic (45) mood states.

Taken together, these studies suggest that striatal and ACC-mediated PE signals, along with mPFC Gln/Glu, are promising biomarkers of reward learning that may be implicated in mood pathology. Therefore, the aim of this study was to determine whether variation in reward learning neurocircuit function predicts variability in symptom trajectories in

individuals with mood disorders. In line with the grant mechanism supporting this study (RFA-MH-14-050; Dimensional Approaches to Research Classification in Psychiatric Disorders), we recruited individuals based on their performance on a well-validated behavioral reward learning task rather than on the basis of specific DSM diagnoses. We then examined whether neurobiological indices of reward learning predicted cross-sectional and longitudinal variation in three reward-relevant symptom domains, namely anhedonia, (hypo)mania, and impulsivity. We predicted that potentiated striatal and ACC-mediated PEs, and elevated mPFC Gln/Glu, would predict worsening (hypo)mania and impulsivity. In contrast, we predicted that blunted striatal and ACC-mediated PEs, and reduced mPFC Gln/Glu, would predict worsening anhedonia. Importantly, we assessed whether these reward learning biomarkers provided superior predictive validity in determining symptom trajectories relative to clinical diagnostic information alone.

METHODS AND MATERIALS

Participants

Subjects in the mood pathology group were required to have depressive, mixed, or hypomanic symptoms severe enough to cause distress/impairment. Participants could pursue treatment but were excluded from further testing if they initiated one of the exclusionary treatments (see [Supplemental Methods](#)). Psychotropic medication load was quantified using previously established procedures ([Supplemental Methods](#)). Subjects in the control group had no lifetime psychiatric disorders or psychotropic medication use. This study was approved by the Partners Human Research Committee. Participants provided written informed consent prior to participating.

Study Design and Recruitment

[Figure 1A](#) shows the study design. Recruitment occurred as follows. Healthy control subjects and treatment-seeking individuals with mood disorders were screened on a probabilistic reward task (PRT) (10,46). Screening continued until two conditions were met: 1) a sample of 32 healthy control subjects with valid PRT data, and who met study eligibility criteria, was recruited and 2) a sample of 80 individuals with mood pathology whose PRT performance spanned the full range of a normative distribution, and who met study eligibility criteria, was recruited. For the 80 individuals with mood pathology, we focused on equally populating quintiles of reward learning ($n \sim 16/\text{quintile}$) ([Figure 2](#)) that were defined using cutoffs derived from a prior normative sample of 572 control subjects who had performed the PRT in prior studies. In total, 272 individuals needed to be screened on the PRT to reach these two criteria (see [Figure S1](#) for study flow diagram).

For participants who were screened on the PRT and had valid data, study eligibility criteria and clinical diagnoses were further evaluated via a Structured Clinical Interview for DSM-IV (47) conducted by master's- or Ph.D.-level interviewers. Participants were also screened with the Young Mania Rating Scale (48) to ensure that at least one third of the mood pathology sample exhibited (hypo)manic symptoms. Eligible

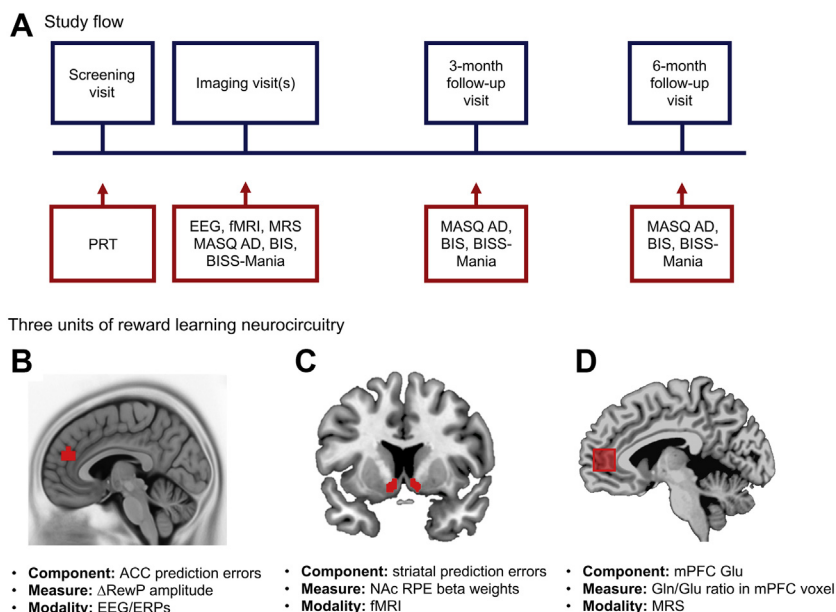


Figure 1. Study methods overview. **(A)** Summary of the study flow. Participants were screened on a probabilistic reward task (PRT), and the patient group was recruited so that patients' scores on the PRT spanned the entire range of possible scores on a preexisting normative distribution. If eligible, a clinical assessment was conducted and then participants returned for two baseline neuroimaging visits (electroencephalography [EEG] and functional magnetic resonance imaging [fMRI]/magnetic resonance spectroscopy [MRS] sessions) as well as 3- and 6-month follow-up assessments. **(B)** Source localization analyses demonstrated that scalp-recorded reward positivity (RewP) amplitude correlated with current source density in the dorsal anterior cingulate cortex (ACC) ($p < .005$ uncorrected; $x = -3$), validating RewP amplitude as a marker of ACC-mediated activation. **(C)** Bilateral nucleus accumbens (NAc) region of interest ($y = 10$) from which striatal reward prediction errors (RPEs) were extracted. **(D)** The $2 \times 2 \times 2$ -cm voxel placed in the medial prefrontal cortex (mPFC) ($x = 0$) from which glutamine/glutamate (Gln/Glu) metabolites were extracted. BIS, Barratt Impulsiveness Scale; BISS-Mania, Mania subscale of the Bipolar Inventory of Symptoms Scale; ERP, event-related potential; MASQ AD, Anhedonic Depression subscale of the Mood and Anxiety Symptom Questionnaire.

participants completed five study visits: 1) behavioral testing and clinical assessment, 2) a baseline EEG/ERP recording, 3) a baseline MRI scan, 4) a 3-month follow-up clinical assessment, and 5) a 6-month follow-up clinical assessment. Participants received \$15/hour in compensation plus earnings on the behavioral and imaging tasks.

Primary Outcomes

Anhedonia was measured using the Anhedonic Depression subscale of the 62-item Mood and Anxiety Symptom Questionnaire (MASQ-AD) (49), and impulsivity was assessed using the Barratt Impulsiveness Scale (BIS) (50). (Hypo)mania was measured using the Mania subscale of the Bipolar Inventory of Symptoms Scale (BISS-mania), which was chosen over the Young Mania Rating Scale because it measures an extended

range of (hypo)manic symptoms (51) and showed greater variance across both unipolar and bipolar groups. These measures were completed at baseline and again at 3- and 6-month follow-up assessments. All three scales demonstrated good internal consistency (Supplemental Methods).

PRT: Quantifying Reward Learning

Reward learning was assessed using a well-validated computer-based PRT (46). On each trial, a fixation cross (500 ms) was followed by a schematic mouthless face (500 ms). Next, a short (11.5-mm) or long (13-mm) mouth appeared (100 ms). Participants indicated whether the mouth was long or short. There were 3 blocks of 100 trials, and for each block 40 correct trials were rewarded ("Correct!! You won 20 cents"). Although long and short mouths were presented at equal frequency,

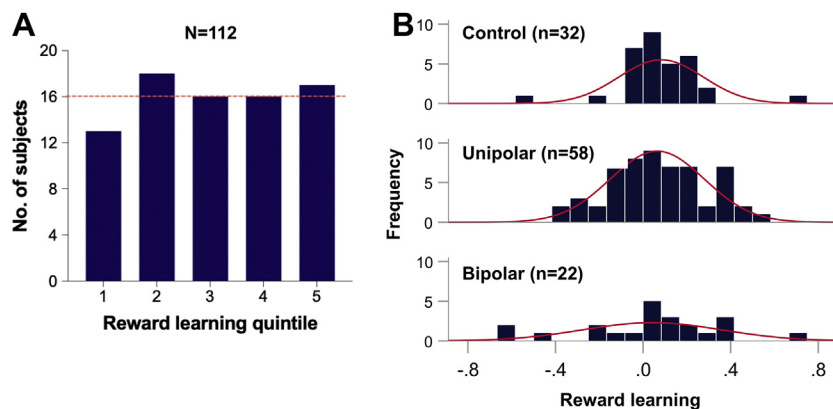


Figure 2. Recruitment based on behavioral reward learning. **(A)** Number of participants with mood pathology whose probabilistic reward task performance fell in each quintile of reward learning performance according to the normative distribution. (The normative distribution was based on a separate existing sample of $N = 572$ healthy control subjects.) The dotted line indicates the a priori target of $n = 16$ per quintile that was set to ensure that we recruited individuals who spanned the entire range of reward learning performance. This target was met in all but the lowest quintile; however, this quintile was still adequately represented with a sample of $n = 13$. **(B)** Frequency histograms of reward learning performance across the control, unipolar, and bipolar groups.

Reward Learning Circuitry in Mood Disorders

unbeknownst to participants, correct identification of one mouth (the rich stimulus) was rewarded 3 times more than the other mouth (the lean stimulus).

Following quality control (Supplemental Methods), we used signal detection analysis (52) to compute response bias (the tendency to bias responding to the rich stimulus) using the following formula:

$$\log b = \frac{1}{2} \log \left(\frac{Rich_{correct} \times Lean_{incorrect}}{Rich_{incorrect} \times Lean_{correct}} \right)$$

To allow calculation of response bias for cases that included a zero in the formula, 0.5 was added to each cell of the matrix (53). Reward learning was defined as the increase in response bias from block 1 to block 3.

Scalp-Recorded RewP Amplitude: Quantifying ACC PEs

The RewP was computed from 128-channel scalp-recorded EEG acquired while participants performed a counterbalanced version of the PRT. After preprocessing, temporospatial principal components analysis (PCA) was used to decompose the time domain ERP (54). Temporal variance in the averaged ERP waveforms was examined using temporal PCA and infomax rotation. Based on the scree plot used to determine the factors to retain in a PCA analysis, 12 temporal factors were retained for rotation. The spatial distribution of these temporal factors was then examined using spatial PCA and infomax rotation, with a spatial PCA being conducted for each temporal factor. Eight spatial factors were retained for each temporal factor. Analyses focused on the PCA component with timing and topography most consistent with the RewP (TF8/SF2; see Supplemental Methods). Furthermore, source localization (55) confirmed that the RewP had a source in the dorsal ACC (Figure 1B). Our primary variable of interest was the difference in RewP amplitude following feedback on lean versus rich trials (Δ RewP), which captures the degree to which the ACC tracks reward probability across different contexts.

fMRI-Based Learning Task: Quantifying Striatal RPEs

Striatal RPE signals were assessed using a well-validated explicit reinforcement learning paradigm (19,56) that required participants to learn reward contingencies through trial and error. On each trial, participants were asked to choose between 2 symbols, where each symbol in the pair was associated with an 80%/20% probability of a given outcome (gain: \$1/\$0; loss: \$0/-\$1; neutral: gray square/nothing). We used Q-learning to calculate the RPE (19) from participants' behavioral data and then imaging analyses focused on a parametric modulation contrast for RPE signals (Supplemental Methods).

Anatomically defined regions of interest in the left and right nucleus accumbens (NAc) were selected from prior research showing links between dopamine transporter function and reward learning (14) (Figure 1C). Beta weights from RPE contrasts were extracted from these regions of interest. A one-sample *t* test confirmed that the RPE in both regions of interest was >0 [left: $t_{106} = 3.07, p = .003$; right: $t_{106} = 4.12, p < .001$], so beta values were averaged to create a single NAc RPE beta weight that was used for subsequent analyses. A positive RPE beta value signified

higher activation for unexpected reward and lower activation for unexpected omission of rewards during gain trials.

MRS: Quantifying mPFC Glutamate

^1H -MRS was used to assess mPFC Gln/Glu. A $2 \times 2 \times 2$ -cm voxel was placed in the mPFC, midsagittally, anterior to the genu of the corpus colosum (Figure 1D). The voxel was automatically shimmed, with further manual shimming performed as needed. A modified J-resolved protocol (57) was used to resolve glutamatergic metabolites. This sequence involved the collection of 22 echo time (TE)-stepped spectra with a TE ranging from 35 to 250 ms in 15-ms increments (repetition time = 2 s, f1 acquisition bandwidth = 67 Hz, spectral bandwidth = 2 kHz, readout duration = 512 ms, number of excitations = 16/TE step, approximate scan duration = 12 min).

To quantify glutamate and glutamine with the modified J-resolved protocol data, the 22 TE-stepped free induction decay series was zero filled out to 64 points, Gaussian filtered, and Fourier transformed using gamma-simulated J-resolved basis sets modeled for 2.89T. Every J-resolved spectral extraction within a bandwidth of 67 Hz was fit with the spectral-fitting package LCModel (<http://s-provencher.com/pages/lcmodel.shtml>) and its theoretically correct template. The integrated area under the entire 2D surface for each metabolite was calculated by summing the raw peak areas across all 64 J-resolved extractions (Supplemental Methods). Our primary outcome was the Gln/Glu ratio.

Statistical Analysis

Multivariable regression analyses examined whether Δ RewP, NAc RPE, or mPFC Gln/Glu predicted anhedonia, (hypo)mania, or impulsivity in the clinical sample cross-sectionally and longitudinally. Separate regression models were run for each outcome (MASQ-AD, BISS-mania, and BIS). Models included covariates (age, sex, and medication load), mood polarity/diagnosis (group: dummy coded with 0 = unipolar and 1 = bipolar), the three neural predictors (Δ RewP, NAc RPE, and mPFC Gln/Glu), and a group \times predictor interaction term for each neural predictor. Models predicting follow-up symptom severity also controlled for baseline symptom severity.

RESULTS

Sample Characteristics

The sample was 63.4% female ($n = 71$), with a mean age of 28.6 years (SD = 9.1, range = 18–60). Of the patient group, 72.5% ($n = 58$) had unipolar mood pathology (MDD/dysthymia or MDD in partial remission), 27.5% ($n = 22$) had bipolar mood pathology (BD type I or II, depressed, mixed, or hypomanic), and 40% ($n = 32$) took medication (see Table 1 and Supplemental Methods for details). Sample sizes for each of the analyses varied when a participant had missing data on one or more of the neural indices and/or follow-up measures. Accordingly, sample sizes ranged from 25 to 32 for the control group, from 38 to 58 for the unipolar group, and from 12 to 22 for the bipolar group (sample sizes for the various analyses are specified below).

Table 1. Demographic and Clinical Characteristics of Sample

	HC (<i>n</i> = 32)	Unipolar (<i>n</i> = 58)	Bipolar (<i>n</i> = 22)	Test	<i>p</i>
Demographic Characteristics					
Age, years, mean (±SD)	28.4 (±7.7)	28.0 (±8.6)	30.5 (±12.1)	<i>F</i> = 0.59	.56
Female, <i>n</i> (%)	17 (53.1)	41 (71.7)	13 (59.1)	$\chi^2 = 2.96$.23
Education, years, mean (±SD)	17.0 (±3.2)	16.0 (±2.8)	15.6 (±3.1)	<i>F</i> = 1.77	.18
White, <i>n</i> (%)	21 (65.6)	40 (69.0)	19 (86.4)	$\chi^2 = 10.02$.26
Hispanic, <i>n</i> (%)	2 (6.3)	6 (10.3)	2 (9.1)	$\chi^2 = 0.43$.81
Clinical Diagnoses, <i>n</i> (%)					
Current MDD	–	49 (84.5)	–	–	–
Current dysthymia	–	1 (1.7)	–	–	–
MDD in partial remission	–	8 (13.8)	–	–	–
BD-I depressed	–	–	7 (31.8)	–	–
BD-I mixed	–	–	0 (0.0)	–	–
BD-I hypomanic	–	–	2 (9.1)	–	–
BD-II depressed	–	–	9 (40.9)	–	–
BD-II mixed	–	–	1 (4.6)	–	–
BD-II hypomanic	–	–	3 (13.6)	–	–
Comorbidities, <i>n</i> (%)					
Alcohol abuse	–	0 (0.0)	2 (9.1)	$\chi^2 = 5.41$.02
EDNOS or BED	–	2 (3.4)	2 (9.1)	$\chi^2 = 1.07$.30
GAD	–	3 (5.2)	2 (9.1)	$\chi^2 = 0.42$.52
Panic disorder	–	1 (1.7)	0 (0.0)	$\chi^2 = 0.38$.54
PTSD	–	3 (5.2)	2 (9.1)	$\chi^2 = 0.42$.52
Social phobia	–	8 (13.8)	3 (13.6)	$\chi^2 = 0.00$.99
Specific phobia	–	3 (5.2)	2 (9.1)	$\chi^2 = 0.42$.52
Medication, <i>n</i> (%)					
Antidepressants	–	19 (32.8)	4 (18.2)	$\chi^2 = 1.65$.20
Mood stabilizer or anticonvulsant	–	1 (1.7)	7 (31.8)	$\chi^2 = 16.05$	<.001
Anticonvulsants	–	0 (0.0)	1 (4.5)	$\chi^2 = 2.67$.10

All tests are two tailed.

BD-I/II, bipolar disorder type I/II; BED, binge eating disorder; EDNOS, eating disorder not otherwise specified; GAD, generalized anxiety disorder; HC, healthy control group; MDD, major depressive disorder; PTSD, posttraumatic-traumatic stress disorder.

Correlations Among Units

Pearson correlations were used to determine the degree to which the three neural indices mapped onto behavioral reward learning (see [Tables S1](#) and [S2](#); differences in units of analysis between diagnostic groups are reported in the [Supplemental Results](#) and [Figure S2](#)). Across the sample, higher mPFC Gln/Glu correlated with better reward learning ($r = .27, p = .007; n = 102$) ([Figure S3A](#)). This was consistent with the linear trend shown in [Figure S3A](#), where mPFC Gln/Glu values increased across the learning quintiles. Furthermore, the quintiles explained a greater proportion of the variance in mPFC Gln/Glu relative to diagnosis (5% vs. 2%; R^2 change = .05, F change = 5.25, $p = .02$).

Although Δ RewP and NAc RPE were not correlated with our a priori–defined learning measure (block 3 minus block 1 response bias), they were correlated with the total overall response bias. Specifically, heightened NAc RPE ($r = .37, p = .04; n = 32$) ([Figure S3B](#)) and Δ RewP ($r = .41, p = .04; n = 25$) ([Figure S3C](#)) correlated with greater overall response bias in control subjects but not in patients ($p > .10, n = 75$). Furthermore, across the whole sample, heightened NAc RPE was associated with faster learning in block 1 ($r = .23, p = .02; n = 107$).

Elevated mPFC Gln/Glu Correlates With More Severe (Hypo)manic Symptoms Cross-Sectionally

Standardized values for each outcome measure across the reward learning quintiles are shown in [Figure S4](#) (patients only). Multimodal regression models assessed whether the three reward circuit markers were associated with symptom severity cross-sectionally.

A significant group \times mPFC Gln/Glu interaction ($\beta = .28, p = .04; n = 57$) emerged from the model predicting baseline (hypo)mania severity (BISS-mania), indicating that the effect of mPFC Gln/Glu on baseline (hypo)mania severity differed across the unipolar and bipolar groups ([Table 2](#)). To unpack this interaction, we examined the correlation between mPFC Gln/Glu and baseline BISS-mania scores (both residualized for other variables in the model) in each group. mPFC Gln/Glu was associated with higher BISS-mania scores in the bipolar group ($r = .56, p = .045; n = 13$) but not in the unipolar group ($r = -.24, p = .12; n = 45$).

In contrast, none of the neural indices predicted anhedonia severity (MASQ-AD) or impulsivity (BIS) (all $ps > .05$) cross-sectionally.

Table 2. Models Predicting (Hypo)manic Symptom Severity on the BISS-mania Scale

	<i>B</i>	SE	β	<i>t</i>	<i>p</i>
Dependent Variable: Baseline (Hypo)manic Symptom Severity					
(Constant)	9.14	2.33		3.92	<.001
Age	-0.09	0.08	-.13	-1.18	.24
Sex	-2.77	1.52	-.20	-1.82	.08
Medication load	-0.71	0.42	-.19	-1.71	.09
Group	10.46	1.60	.69	6.52	<.001
Δ RewP	-0.70	1.24	-.07	-0.56	.58
NAc RPE	0.03	0.57	.01	0.05	.96
mPFC Gln/Glu	-9.33	16.39	-.07	-0.57	.57
Group \times Δ RewP	-1.48	2.27	-.09	-0.65	.52
Group \times NAc RPE	2.11	1.90	.13	1.11	.27
Group \times mPFC Gln/Glu	68.06	31.51	.28	2.16	.04
Dependent Variable: 3-Month (Hypo)manic Symptom Severity					
(Constant)	3.49	1.93		1.81	.08
Age	0.06	0.06	.15	0.99	.33
Sex	-2.14	1.19	-.27	-1.80	.08
Medication load	-0.29	0.32	-.12	-0.90	.37
Baseline BISS-mania	0.16	0.11	.28	1.54	.13
Group	-1.15	1.61	-.13	-0.71	.48
Δ RewP	-1.02	0.99	-.16	-1.03	.31
NAc RPE	-0.04	0.43	-.01	-0.10	.92
mPFC Gln/Glu	-38.43	14.30	-.46	-2.69	.01
Group \times Δ RewP	1.03	1.93	.08	0.53	.60
Group \times NAc RPE	-0.07	1.35	-.01	-0.05	.96
Group \times mPFC Gln/Glu	96.92	24.90	.70	3.89	<.001

Group was dummy coded (0 = unipolar, 1 = bipolar).

BISS-mania, Mania subscale score of Bipolar Inventory of Symptoms Scale; RewP, reward positivity; NAc RPE, nucleus accumbens reward prediction error; mPFC Gln/Glu, medial prefrontal cortex ratio of glutamine to glutamate.

Elevated mPFC Gln/Glu Correlates With More Severe (Hypo)manic Symptoms Longitudinally

Next, we examined whether, after controlling for baseline (hypo)manic severity, the reward circuit markers were associated with 3- and 6-month follow-up symptom severity (see [Figure S5](#) for mean symptom severity across time). A group \times mPFC Gln/Glu interaction ($\beta = .70, p < .001; n = 49$) emerged for the model predicting 3-month BISS-mania scores ([Table 2](#)). To unpack this interaction, we again examined the correlation between mPFC Gln/Glu and 3-month BISS-mania scores (residualized for other variables in the model) in each group. Increased mPFC Gln/Glu was associated with less severe hypomanic symptoms in the unipolar group ($r = -.35, p = .03; n = 38$) but with more severe hypomanic symptoms in the bipolar group ($r = .85, p < .001; n = 12$) ([Figure 3](#)) at 3 months.

In contrast, the reward learning markers did not predict 6-month follow-up BISS-mania scores or 3- or 6-month MASQ-AD or BIS scores (all $ps > .05$) (see [Supplemental Results](#) for exploratory unimodal analyses).

Predictive Value of mPFC Gln/Glu

Next, we compared a simple model containing covariates (age, sex, medication load, and baseline BISS-mania) and

diagnostic information (group) with a model containing terms for mPFC Gln/Glu and group \times mPFC Gln/Glu. The simple model explained 15.8% of the variance in 3-month (hypo)manic symptom severity, $F_{5,44} = 1.65, p = .17$. However, adding the mPFC Gln/Glu terms explained an additional 24.3% of the variance in 3-month hypomanic symptom severity, $F_{7,42} = 4.01, p = .002$, and this change in R^2 was significant (F change = 8.49, R^2 change = .24, $p = .001$). This indicates that mPFC Gln/Glu explained greater variance in future hypomanic symptom severity relative to baseline diagnosis alone. Furthermore, we confirmed that mPFC Gln/Glu explained a greater proportion of the variance in 3-month (hypo)manic symptom severity relative to behavioral reward learning alone (F change = 3.91, R^2 change = .09, $p = .03$) ([Table S3](#)), indicating that adding this biomarker enhanced predictive power over and above behavioral data.

DISCUSSION

Using a novel recruitment method, a transdiagnostic sample, and a multimodal longitudinal design, we examined whether variation along the RDoC Positive Valence Systems domain of reward learning and the underlying neurocircuitry predicted variability in three reward-related mood symptoms: anhedonia, (hypo)mania, and impulsivity. In doing so, we focused on three components of reward learning neurocircuitry linked to mood disorder pathophysiology that span distinct units of analysis across physiology (ACC-mediated PEs), circuits (striatal RPEs), and molecules (mPFC Gln/Glu).

As predicted, the three neural components correlated with aspects of behavioral reward learning on the PRT. In terms of symptoms, elevated mPFC Gln/Glu predicted more severe cross-sectional and longitudinal (hypo)manic symptoms in those with bipolar pathology. Importantly, baseline mPFC Gln/Glu levels explained a greater proportion of the variance in (hypo)manic symptoms at 3 months relative to diagnosis alone. These findings extend prior case-control MRS studies ([41,42](#)) by showing that elevated mPFC Gln/Glu is also associated with (hypo)mania severity dimensionally.

We replicated prior findings linking blunted Δ RewP amplitude with greater anhedonia in exploratory unimodal analyses (see [Supplement](#)); however, neither Δ RewP nor NAc RPE signals were associated with symptom severity when entered into a multimodal model with mPFC Gln/Glu. Although the lack of a relationship between NAc RPE and anhedonia in our unimodal analyses contrasts with recent findings showing that striatal RPEs predicted improvement in anhedonic symptoms ([58](#)), we used a more complex instrumental fMRI learning paradigm designed to assess striatal RPEs in the context of learning as opposed to a more traditional guessing-type paradigm (which maximizes the RPE signal yet involves minimal learning).

It is important to consider what these findings mean for an RDoC approach to mood disorder classification that remains agnostic to DSM diagnoses. On the one hand, mPFC Gln/Glu correlated with reward learning across diagnoses, providing converging evidence that mPFC Gln/Glu is a transdiagnostic marker of this RDoC domain. In addition, in a heterogeneous

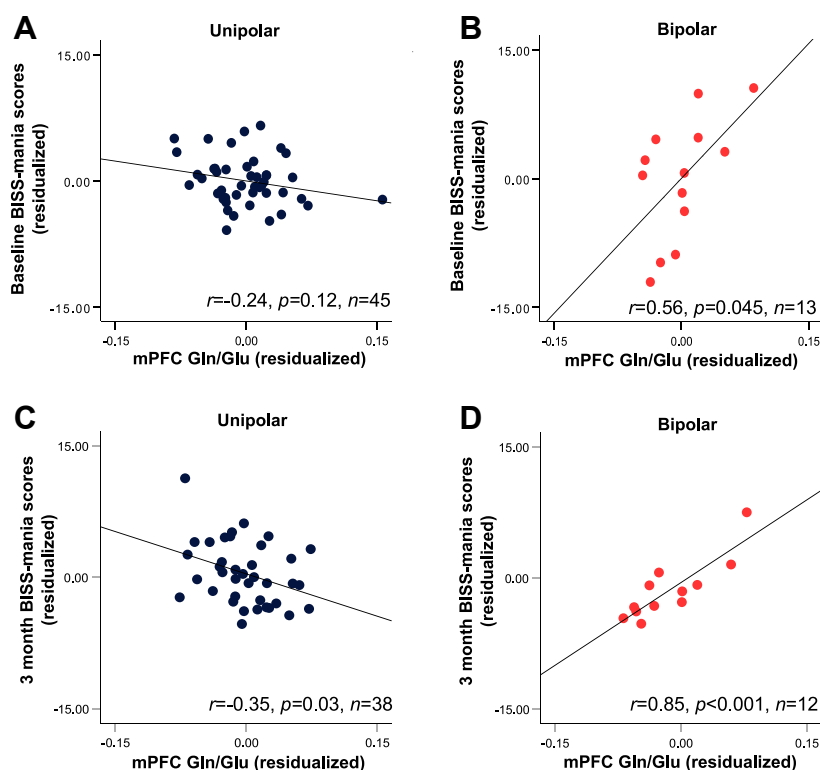


Figure 3. Group \times medial prefrontal cortex (mPFC) glutamine/glutamate (Gln/Glu) interaction for longitudinal (hypo)manic symptom severity. Residualized scatter plots show the relationship between mPFC Gln/Glu and (hypo)manic symptom severity (Mania subscale scores of the Bipolar Inventory of Symptoms Scale [BISS-mania]) at baseline (**A, B**) and at the 3-month follow-up assessment (**C, D**) in the unipolar and bipolar mood disorder groups. Residualized values on each axis control for the other variables in the model, which were age, sex, baseline BISS-mania subscale scores, change in reward positivity amplitude, and nucleus accumbens reward prediction error beta weights.

sample, more homogeneity in neurobiology (mPFC Gln/Glu levels) was observed within groups when groups were defined on the basis of reward learning versus diagnostic categories. This is consistent with the RDoC's assumption that dimensions of functioning are more proximal to neurobiology than to diagnostic categories. Furthermore, dimensional increases in this reward learning biomarker (i.e., mPFC Gln/Glu levels) predicted dimensional increases in symptoms characterized by excessive reward responsiveness (i.e., hypomania) rather than membership in a specific diagnostic category. This echoes one of the RDoC's central theses that abnormalities in circuits and associated constructs likely underpin specific features of mental illness rather than explain any single disorder in its entirety. Together, these findings partly align with a diagnosis-agnostic approach to mood disorder classification.

However, our results also highlight the considerable value of diagnostic information in predicting symptom trajectories. Specifically, although mPFC Gln/Glu correlated with reward learning transdiagnostically, the link between mPFC Gln/Glu and (hypo)manic symptom severity was disease specific and diagnostic information remained an integral component of the final predictive model. If we assume that these findings could inform novel interventions based on neurobiological underpinnings (a key driver of the RDoC approach), then targeting mPFC Gln/Glu may affect reward learning in a similar manner across disorders but have different effects on symptoms in distinct mood disorder subtypes. The degree to which the RDoC framework predicts purely dimensional variability

across disorders versus a blend of transdiagnostic and disorder-specific effects remains an important topic of debate. Our findings indicate that while information about reward circuit function could improve the prediction of risk for reward-related clinical symptoms (an important finding in its own right), it would do so in tandem with, rather than independent of, existing diagnostic frameworks.

This study has several strengths. By examining neurobiological mechanisms of reward learning across multiple units of analysis, we could probe reward learning circuitry with superior spatiotemporal resolution and at both micro and macro scales, which cannot be achieved with a single unit or modality alone. Furthermore, we tested whether these units of analysis enhanced the ability to predict clinical course over and above information already used in routine clinical care (diagnosis and baseline symptom severity). Because mPFC Gln/Glu levels can be obtained using MRS in as little as 6 minutes with good test-retest reliability (intraclass correlation coefficient = .803) (59), mPFC Gln/Glu warrants further investigation as a potential screening method for individuals at suspected risk for BD.

However, some limitations of this study must also be noted. First, mPFC Gln/Glu predicted worse (hypo)manic symptoms specifically in individuals with bipolar mood pathology. Because the instance of (hypo)manic symptoms was lower in the unipolar group at follow-up, this may have restricted the variance in symptoms that could be explained by mPFC Gln/Glu. Second, although our three neural indices were selected based on their established association with reward learning,

Reward Learning Circuitry in Mood Disorders

only mPFC Gln/Glu was associated with our a priori reward learning measure and the three neural indices were not correlated with one another. Although stronger associations may have been evident in a larger sample, the lack of association could also reflect an issue with the construct validity of these units of analysis. For example, it is possible that similar impairments in reward learning may have distinct etiologies (often referred to as equifinality), particularly when considering individuals with very divergent forms of psychopathology. How equifinality is accounted for remains an important conceptual issue for the RDoC framework. Finally, reductions in sample size for longitudinal analyses (resulting from participant attrition and the need to obtain good quality data across all three neural indices) mean that reduced statistical power is a limitation of our study and may explain several null findings. The replicability of these results must be interpreted in light of concerns around the generalizability and reproducibility of neuroimaging findings obtained using small samples (60). Accordingly, rather than being definitive, we interpret these findings as novel yet preliminary insights that warrant replication in larger samples.

In sum, we showed that a key component of reward learning neurocircuitry—mPFC Gln/Glu—predicted worse (hypo)manic symptoms. This marker enhanced the ability to predict future (hypo)mania risk over and above diagnostic information alone. Using this marker to improve precision in the diagnosis and treatment of mood pathology therefore represents an important avenue for future research, with a focus on larger well-powered samples.

ACKNOWLEDGMENTS AND DISCLOSURES

This project was supported by the National Institute of Mental Health (NIMH) (Grant Nos. R01 MH101521 and R37 MH068376 [to DAP]). AEW received support from the National Health and Medical Research Council (Grant No. GNT1110773).

The content is solely the responsibility of the authors and does not necessarily represent the official views of the National Institutes of Health. The funding organizations had no role in the design and conduct of the study; collection, management, analysis, and interpretation of the data; the preparation, review, or approval of the manuscript; and the decision to submit the manuscript for publication.

AEW, PK, and DAP had full access to all the data in the study and take responsibility for the integrity and accuracy of the data. DAP, MTT, and AEW were responsible for study concept and design. AEW was responsible for drafting the manuscript. AEW, DAP, MTT, PK, DF, FD, MLI, and AVR were responsible for critical revision of the manuscript for important intellectual content. AEW, PK, DF, and GF were responsible for statistical analysis. MLI, AVR, and FD were responsible for administrative, technical, or material support. DAP and AEW were responsible for study supervision.

We acknowledge Thilo Deckersbach, Andrew Nierenberg, and Amy Farabaugh for facilitating recruitment of participants through the Depression Clinic and Research Program and the Bipolar Clinic and Research Program at Massachusetts General Hospital and also acknowledge Daniel Ju Hyung Kim, Emily E. Bernstein, and Margaret E. Gigler for their assistance with patient screening and data collection at these two clinics. We also thank Madeline M. Alexander, Laurie A. Scott, Nancy Hall-Brooks, and David J. Crowley for their important contributions to the screening and clinical assessment of participants recruited through the McLean Hospital Center for Depression, Anxiety and Stress Research. Finally, we recognize the critical contributions of J. Eric Jensen, who passed away while this study was being conducted. Dr. Jensen's expertise was integral to the design and implementation of the MRS protocol used in the current study, and this article is dedicated to him.

The findings from this study were presented in part as posters or invited talks at the 2015 (Toronto, Ontario, Canada) and 2019 (Chicago, Illinois) Social of Biological Psychiatry annual meetings, the 2015 (Miami, Florida) and 2017 (San Francisco, California) Anxiety and Depression Association of America annual meetings, and the 2017 (Boston, Massachusetts) Association for Psychological Science annual meeting.

Over the past 3 years, DAP has received funding from the NIMH, the Brain and Behavior Research Foundation, the Dana Foundation, and Millennium Pharmaceuticals; consulting fees from BlackThorn Therapeutics, Boehringer Ingelheim, Compass Pathway, Concert Pharmaceuticals, Engrail Therapeutics, Neurocrine Biosciences, Otsuka Pharmaceuticals, and Takeda Pharmaceuticals; one honorarium from Alkermes; and stock options from BlackThorn Therapeutics. DAP has a financial interest in BlackThorn Therapeutics, which has licensed the copyright to the PRT through Harvard University. DAP's interests were reviewed and are managed by McLean Hospital and Partners HealthCare in accordance with their conflict of interest policies. All other authors report no biomedical financial interests or potential conflicts of interest.

ClinicalTrials.gov: Brain Mechanisms of Human Motivation; <https://clinicaltrials.gov/ct2/show/NCT01976975>; NCT01976975.

ARTICLE INFORMATION

From the Center for Depression, Anxiety and Stress Research (AEW, PK, AVR, MLI, GF, FD, DAP), McLean Hospital, Belmont, and Department of Psychiatry (AEW, PK, AVR, MLI, GF, FD, DAP), Harvard Medical School, Boston, Massachusetts; Department of Psychology (MTT), Emory University, Atlanta, Georgia; Department of Psychological Sciences (DF), Purdue University, West Lafayette, Indiana; and Black Dog Institute (AEW), University of New South Wales, Randwick, New South Wales, Australia.

Address correspondence to Diego A. Pizzagalli, Ph.D., at dap@mclean.harvard.edu.

Received Nov 12, 2020; revised Dec 25, 2020; accepted Jan 7, 2021.

Supplementary material cited in this article is available online at <https://doi.org/10.1016/j.bpsc.2021.01.004>.

REFERENCES

1. American Psychiatric Association (2013): *Diagnostic and Statistical Manual of Mental Disorders*, 5th ed. Washington, DC: American Psychiatric Publishing.
2. World Health Organization (2018): *International Classification of Diseases for Mortality and Morbidity Statistics*, 11th revision Geneva, Switzerland: World Health Organization.
3. Yatham LN, Kennedy SH, Parikh SV, Schaffer A, Bond DJ, Frey BN, et al. (2018): Canadian Network for Mood and Anxiety Treatments (CANMAT) and International Society for Bipolar Disorders (ISBD) 2018 guidelines for the management of patients with bipolar disorder. *Bipolar Disord* 20:97–170.
4. Goodwin G, Haddad P, Ferrier I, Aronson J, Barnes T, Cipriani A, et al. (2016): Evidence-based guidelines for treating bipolar disorder: Revised third edition recommendations from the British Association for Psychopharmacology. *J Psychopharmacol* 30:495–553.
5. Cuthbert BN, Insel TR (2013): Toward the future of psychiatric diagnosis: The seven pillars of RDoC. *BMC Med* 11:126.
6. Cuthbert BN (2014): The RDoC framework: Facilitating transition from ICD/DSM to dimensional approaches that integrate neuroscience and psychopathology. *World Psychiatry* 13:28–35.
7. Whitton AE, Treadway MT, Pizzagalli DA (2015): Reward processing dysfunction in major depression, bipolar disorder and schizophrenia. *Curr Opin Psychiatry* 28:7–12.
8. Alloy LB, Nusslock R, Boland EM (2015): The development and course of bipolar spectrum disorders: An integrated reward and circadian rhythm dysregulation model. *Annu Rev Clin Psychol* 11:213–250.
9. Pizzagalli DA, Goetz E, Ostacher M, Iosifescu DV, Perlis RH (2008): Euthymic patients with bipolar disorder show decreased reward learning in a probabilistic reward task. *Biol Psychiatry* 64:162–168.

10. Pizzagalli DA, Iosifescu D, Hallett LA, Ratner KG, Fava M (2008): Reduced hedonic capacity in major depressive disorder: Evidence from a probabilistic reward task. *J Psychiatric Res* 43:76–87.
11. Vrieze E, Pizzagalli DA, Demyttenaere K, Hompes T, Sienaert P, de Boer P, *et al.* (2013): Reduced reward learning predicts outcome in major depressive disorder. *Biol Psychiatry* 73:639–645.
12. Pizzagalli DA, Evins AE, Schetter EC, Frank MJ, Pajtas PE, Santesso DL, Culhane M (2008): Single dose of a dopamine agonist impairs reinforcement learning in humans: Behavioral evidence from a laboratory-based measure of reward responsiveness. *Psychopharmacology* 196:221–232.
13. Santesso DL, Evins AE, Frank MJ, Schetter EC, Bogdan R, Pizzagalli DA (2009): Single dose of a dopamine agonist impairs reinforcement learning in humans: Evidence from event-related potentials and computational modeling of striatal-cortical function. *Hum Brain Mapp* 30:1963–1976.
14. Kaiser RH, Treadway MT, Wooten DW, Kumar P, Goer F, Murray L, *et al.* (2018): Frontostriatal and dopamine markers of individual differences in reinforcement learning: A multi-modal investigation. *Cereb Cortex* 28:4281–4290.
15. Bogdan R, Pizzagalli DA (2009): The heritability of hedonic capacity and perceived stress: A twin study evaluation of candidate depressive phenotypes. *Psychol Med* 39:211–218.
16. Schultz W (2015): Neuronal reward and decision signals: From theories to data. *Physiol Rev* 95:853–951.
17. Balleine BW, O'Doherty JP (2010): Human and rodent homologies in action control: Corticostriatal determinants of goal-directed and habitual action. *Neuropsychopharmacology* 35:48–69.
18. Daw ND, Niv Y, Dayan P (2005): Uncertainty-based competition between prefrontal and dorsolateral striatal systems for behavioral control. *Nat Neurosci* 8:1704–1711.
19. Pessiglione M, Seymour B, Flandin G, Dolan RJ, Frith CD (2006): Dopamine-dependent prediction errors underpin reward-seeking behaviour in humans. *Nature* 442:1042–1045.
20. Schultz W, Dayan P, Montague PR (1997): A neural substrate of prediction and reward. *Science* 275:1593–1599.
21. Gläscher J, Daw N, Dayan P, O'Doherty JP (2010): States versus rewards: Dissociable neural prediction error signals underlying model-based and model-free reinforcement learning. *Neuron* 66:585–595.
22. Schultz W (2016): Dopamine reward prediction-error signalling: A two-component response. *Nat Rev Neurosci* 17:183–195.
23. Kumar P, Goer F, Murray L, Dillon DG, Beltzer ML, Cohen AL, *et al.* (2018): Impaired reward prediction error encoding and striatal-midbrain connectivity in depression. *Neuropsychopharmacology* 43:1581–1588.
24. Whitton AE, Reinen JM, Slifstein M, Ang Y-S, McGrath PJ, Iosifescu DV, *et al.* (2020): Baseline reward processing and ventrostriatal dopamine function are associated with pramipexole response in depression. *Brain* 143:701–710.
25. Kumar P, Waiter G, Ahearn T, Milders M, Reid I, Steele J (2008): Abnormal temporal difference reward-learning signals in major depression. *Brain* 131:2084–2093.
26. Nusslock R, Almeida JR, Forbes EE, Versace A, Frank E, LaBarbara EJ, *et al.* (2012): Waiting to win: Elevated striatal and orbitofrontal cortical activity during reward anticipation in euthymic bipolar disorder adults. *Bipolar Disord* 14:249–260.
27. O'Sullivan N, Szczepanowski R, El-Deredy W, Mason L, Bental RP (2011): fMRI evidence of a relationship between hypomania and both increased goal-sensitivity and positive outcome-expectancy bias. *Neuropsychologia* 49:2825–2835.
28. Abler B, Greenhouse I, Ongur D, Walter H, Heckers S (2008): Abnormal reward system activation in mania. *Neuropsychopharmacology* 33:2217–2227.
29. Proudfit GH (2015): The reward positivity: From basic research on reward to a biomarker for depression. *Psychophysiology* 52:449–459.
30. Foti D, Weinberg A, Dien J, Hajcak G (2011): Event-related potential activity in the basal ganglia differentiates rewards from nonrewards: Response to commentary. *Hum Brain Mapp* 32:2267–2269.
31. Santesso DL, Dillon DG, Birk JL, Holmes AJ, Goetz E, Bogdan R, Pizzagalli DA (2008): Individual differences in reinforcement learning: Behavioral, electrophysiological, and neuroimaging correlates. *NeuroImage* 42:807–816.
32. Whitton AE, Kakani P, Foti D, Van't Veer A, Haile A, Crowley DJ, Pizzagalli DA (2016): Blunted neural responses to reward in remitted major depression: A high-density event-related potential study. *Biol Psychiatry Cogn Neurosci Neuroimaging* 1:87–95.
33. Mason L, O'Sullivan N, Blackburn M, Bental R, El-Deredy W (2012): I want it now! Neural correlates of hypersensitivity to immediate reward in hypomania. *Biol Psychiatry* 71:530–537.
34. Foti D, Hajcak G (2009): Depression and reduced sensitivity to non-rewards versus rewards: Evidence from event-related potentials. *Biol Psychol* 81:1–8.
35. Bress JN, Foti D, Kotov R, Klein DN, Hajcak G (2013): Blunted neural response to rewards prospectively predicts depression in adolescent girls. *Psychophysiology* 50:74–81.
36. Holroyd CB, Coles MG (2002): The neural basis of human error processing: Reinforcement learning, dopamine, and the error-related negativity. *Psychol Rev* 109:679–709.
37. Geisler S, Derst C, Veh RW, Zahm DS (2007): Glutamatergic afferents of the ventral tegmental area in the rat. *J Neurosci* 27:5730–5743.
38. Hauber W, Sommer S (2009): Prefrontostriatal circuitry regulates effort-related decision making. *Cereb Cortex* 19:2240–2247.
39. Jocham G, Hunt LT, Near J, Behrens TE (2012): A mechanism for value-guided choice based on the excitation-inhibition balance in prefrontal cortex. *Nat Neurosci* 15:960–961.
40. Pellerin L, Magistretti PJ (2004): Let there be (NADH) light. *Science* 305:50–52.
41. Yüksel C, Öngür D (2010): Magnetic resonance spectroscopy studies of glutamate-related abnormalities in mood disorders. *Biol Psychiatry* 68:785–794.
42. Gigante AD, Bond DJ, Lafer B, Lam RW, Young LT, Yatham LN (2012): Brain glutamate levels measured by magnetic resonance spectroscopy in patients with bipolar disorder: A meta-analysis. *Bipolar Disord* 14:478–487.
43. Öngür D, Jensen JE, Prescott AP, Stork C, Lundy M, Cohen BM, Renshaw PF (2008): Abnormal glutamatergic neurotransmission and neuronal-glia interactions in acute mania. *Biol Psychiatry* 64:718–726.
44. Frye MA, Watzl J, Banakar S, O'Neill J, Mintz J, Davanzo P, *et al.* (2007): Increased anterior cingulate/medial prefrontal cortical glutamate and creatine in bipolar depression. *Neuropsychopharmacology* 32:2490–2499.
45. Kubo H, Nakataki M, Sumitani S, Iga J-I, Numata S, Kameoka N, *et al.* (2017): ¹H-magnetic resonance spectroscopy study of glutamate-related abnormality in bipolar disorder. *J Affect Disord* 208:139–144.
46. Pizzagalli DA, Jahn AL, O'Shea JP (2005): Toward an objective characterization of an anhedonic phenotype: A signal-detection approach. *Biol Psychiatry* 57:319–327.
47. First MB, Spitzer RL, Gibbon M, Williams JB (2002): Structured Clinical Interview for DSM-IV-TR Axis I Disorders, Research Version, Patient Edition (SCID-I/P). New York: New York State Psychiatric Institute.
48. Young RC, Biggs JT, Ziegler VE, Meyer DA (1978): A rating scale for mania: Reliability, validity and sensitivity. *Br J Psychiatry* 133:429–435.
49. Watson D, Weber K, Assenheimer JS, Clark LA, Strauss ME, McCormick RA (1995): Testing a tripartite model: I. Evaluating the convergent and discriminant validity of anxiety and depression symptom scales. *J Abnorm Psychol* 104:3–14.
50. Patton JH, Stanford MS, Barratt ES (1995): Factor structure of the Barratt Impulsiveness Scale. *J Clin Psychol* 51:768–774.
51. Gonzalez JM, Bowden CL, Katz MM, Thompson P, Singh V, Prihoda TJ, Dahl M (2008): Development of the Bipolar Inventory of Symptoms Scale: Concurrent validity, discriminant validity and retest reliability. *Int J Methods Psychiatr Res* 17:198–209.
52. Macmillan N, Creelman C (1991): Detection Theory: A User's Guide. Cambridge, UK: Cambridge University Press.
53. Hautus MJ (1995): Corrections for extreme proportions and their biasing effects on estimated values of *d'*. *Behav Res Methods Instrum Comput* 27:46–51.

Reward Learning Circuitry in Mood Disorders

54. Dien J (2010): The ERP PCA Toolkit: An open source program for advanced statistical analysis of event-related potential data. *J Neurosci Methods* 187:138–145.
55. Pascual-Marqui RD (2002): Standardized low-resolution brain electromagnetic tomography (sLORETA): Technical details. *Methods Find Exp Clin Pharmacol* 24:5–12.
56. Treadway MT, Admon R, Arulpragasam AR, Mehta M, Douglas S, Vitaliano G, *et al.* (2017): Association between interleukin-6 and striatal prediction-error signals following acute stress in healthy female participants. *Biol Psychiatry* 82:570–577.
57. Brennan BP, Tkachenko O, Schwab ZJ, Juelich RJ, Ryan EM, Athey AJ, *et al.* (2015): An examination of rostral anterior cingulate cortex function and neurochemistry in obsessive–compulsive disorder. *Neuropsychopharmacology* 40:1866–1876.
58. Eckstrand KL, Forbes EE, Bertocci MA, Chase HW, Greenberg T, Lockovich J, *et al.* (2019): Anhedonia reduction and the association between left ventral striatal reward response and 6-month improvement in life satisfaction among young adults. *JAMA Psychiatry* 8:958–965.
59. Jensen JE, Auerbach RP, Pisoni A, Pizzagalli DA (2017): Localized MRS reliability of in vivo glutamate at 3 T in shortened scan times: A feasibility study. *NMR Biomed* 30:e3771.
60. Sui J, Jiang R, Bustillo J, Calhoun VJBP (2020): Neuroimaging-based individualized prediction of cognition and behavior for mental disorders and health: Methods and promises. *Biol Psychiatry* 88:818–828.

**Pretreatment Rostral Anterior Cingulate Cortex Connectivity
With Salience Network Predicts Depression Recovery:
Findings from the EMBARC Randomized Clinical Trial**

Supplementary Information

Contents:

Supplementary Methods
Supplementary Results
Figures S1, S2, S3 and S4
Tables S1, S2, S3, and S4
Supplementary References

Supplementary Methods and Materials

Sample size and power analyses for the clinical trial

The sample size of 300 was chosen to allow at least 80% power ($\alpha=0.05$, two-tailed) to detect interaction effects of multiple (~40) potential moderators of the treatment on depressive symptom improvement, after adjusting for multiple comparisons. Based on prior work, the effect sizes of the moderators were hypothesized to be between 0.15 and 0.2.

Methods used to generate the random allocation sequence

Randomization was conducted according to site, depression severity and depression chronicity. Within each of these levels, block randomization with a random block size of 2 or 4 was applied using the commercial clinical trial data management software StudyTrax. For each potential participant, a site coordinator would input information regarding all inclusion/exclusion criteria, after which the software crosschecked this information for eligibility. If the participant was deemed to be eligible, the software provided a random assignment, which was communicated directly to the site pharmacist.

Participant inclusion/exclusion criteria

All patients reported MDD onset before 30, and had either a chronic (episode duration > 2 years) or recurrent (≥ 2 recurrences including the current episode) illness course. Participants were excluded from the study if they were currently pregnant, breastfeeding or were planning to become pregnant in the near future; had a lifetime history of bipolar disorder or psychotic disorder; met criteria for substance dependence in the past six months or substance abuse in the past two months; displayed evidence of unstable medical or psychiatric symptoms that required hospitalization; had any study medication contraindications; had clinically significant laboratory abnormalities; had a

history of epilepsy or any condition requiring anticonvulsant medication; had received transcranial magnetic stimulation, vagal nerve stimulation or electroconvulsive therapy during the current depressive episode; were currently taking psychotropic medications; were currently receiving psychotherapy; displayed evidence of significant suicide risk; failed to respond to any antidepressant at adequate dose and duration in the current episode.

Participant compensation

Compensation for the study components relevant to the current analyses was as follows:

- Completion of the detailed interview and questionnaires administered at screening – \$150
- Completion of the two EEG recordings – \$68

Compensation for other study components that are not presented in this study, was as follows:

- Completion of two MRI scans – up to \$200
- Completion of a behavioral task – up to \$32
- Completion of blood samples for research purposes – \$25 per sample, up to \$175 total
- Completion of genetic blood sampling – \$50
- Completion of the final clinical rating session of the study – \$50

The total possible compensation for the study was \$725.

Participants lost to follow-up

Of the 143 participants who received sertraline, 117 completed all 8 weeks of the intervention, whereas 26 discontinued (7 of whom were lost to follow-up). Of the 144 participants who received placebo, 125 completed all 8 weeks of the intervention, whereas 19 discontinued (5 of whom were lost to follow-up). A summary of the reasons why participants dropped out is provided in Table S1.

EEG systems used across the four recording sites

Columbia University. 72-channel EEG was recorded using a 24-bit BioSemi system with a Lycra stretch electrode cap (Electro-Cap International Inc., Ohio), sampled at 256 Hz (bandpass: DC-

251.3 Hz). An active reference (ActiveTwo EEG system) at electrode locations PPO1 (common mode sense) and PPO2 (driven right leg) were used.

McLean Hospital. 129-channel EEG was recorded using a Geodesic Sensor Net system (Electrical Geodesics, Inc., Eugene, Oregon), sampled at 250 Hz (bandpass: 0.01-100 Hz). Data were referenced to the vertex (Cz) at acquisition.

University of Michigan. 60-channel EEG was recorded using a 32-bit NeuroScan Synamp system (Compumedics, TX) using a Lycra stretch electrode cap (Electro-Cap International Inc., Ohio), sampled at 250 Hz (bandpass: 0.5-100 Hz). A nose reference was used during acquisition.

University of Texas. 62-channel EEG was recorded using a 32-bit Neuroscan Synamp system (Compumedics, TX) using a Lycra stretch electrode cap (Electro-Cap International Inc., Ohio), sampled at 250 Hz (bandpass: DC-100 Hz). A nose reference was used during acquisition.

EEG preprocessing

A standardized analysis pipeline was developed and implemented by researchers at the Columbia site to minimize cross-site differences (1). First, data were interpolated to a common, 72-channel montage using spherical spline (2) and resampled at 256 Hz. Second, electrodes with poor signal were interpolated using a spherical spline interpolation (recordings with less than 80% of usable data were discarded). Third, a spatial principal component analysis was used to correct for blink artifacts (3). Fourth, artifact-free data were segmented into 2 second, non-overlapping epochs, and bandpass filtered at 1-60 Hz (24-dB/octave). Fifth, residual artifacts were identified on an individual channel basis within each epoch using a semiautomated reference-free approach (4). Finally, flagged channels were interpolated using spherical spline from data of all valid channels for a given epoch if less than 25% of channels were flagged for this epoch.

Evidence for the validity of the LORETA algorithm

The eLORETA solution space consists of 6239 cortical gray matter voxels in a realistic head model using the Montreal Neurological Institute 152 template. Validation for the LORETA algorithm comes from studies using simultaneous EEG and fMRI (5) as well as in an EEG localization study for epilepsy (6). The algorithm has also received validation from studies examining LORETA and fMRI data (7-9), or LORETA and PET data (10-12) in the same samples. In a review of independent source localization techniques, sLORETA – the algorithm upon which the eLORETA algorithm used in the current study was based – was found to perform best in terms of localization error (13). In the context of functional connectivity, eLORETA has been found to minimize the detection of false positive connections significantly more so compared to other EEG source localization methods (14).

Additional information about computation of lagged phase synchronization

Lagged phase synchronization is a metric that refers to the nonlinear dependence between the phases of pairs of intracortical EEG source estimates. It is a measure of phase synchrony between intracortical signals in the frequency domain (calculated using normalized Fourier transforms). The strength of this method is its ability to minimize the impact of volume conduction on EEG source-based connectivity estimates. Specifically, volume conduction refers to the tendency for intracortical signals to spread laterally upon contact with the skull, and this causes spurious correlations in activity detected at neighboring scalp-level electrodes. To minimize the effects of volume conduction, the instantaneous “zero-lag” contribution is excluded from the total phase synchronization, leaving only non-instantaneous synchronization.

Total phase synchronization (which is susceptible to volume conduction effects) is typically computed using the following formula:

$$\varphi^2_{x,y}(\omega) = |f_{x,y}(\omega)|^2 = \{\text{Re}[f_{x,y}(\omega)]\}^2 + \{\text{Im}[f_{x,y}(\omega)]\}^2 \quad (1)$$

$$\text{where: } f_{x,y}(\omega) = \frac{1}{N_R} \sum_{k=1}^{N_R} \left[\frac{x_k(\omega)}{|x_k(\omega)|} \right] \left[\frac{y_k^*(\omega)}{|y_k(\omega)|} \right] \quad (2)$$

In this algorithm, “ ω ” refers to the frequency band, and “ x ” and “ y ” are the intracortical sources (i.e., two ROIs in each connectivity pair). “Re” and “Im” indicate the real and the imaginary parts of a complex element C , respectively; $x(\omega)$ and $y(\omega)$ denote the Fourier transforms of the two signals x and y , respectively, at frequency “ ω ”.

The second part of the formula (2) explains the cycle of C and “*” denotes a complex conjugate (this is where the sign of the imaginary part of a complex number is flipped but the real part is left unchanged). The instantaneous connectivity component is closely related to the real (“Re”) part of the phase synchronization.

Lagged phase synchronization partials out the instantaneous component of total connectivity, and is defined as:

$$\varphi^2_{x,y}(\omega) = \frac{\{\text{Im}[f_{x,y}(\omega)]\}^2}{1 - \{\text{Re}[f_{x,y}(\omega)]\}^2} \quad (3)$$

This measures the similarity of two time series according to the phases of the signal, after the instantaneous similarity has been removed. A value of 0 indicates no synchronization and 1 indicates perfect synchronization. This measure is thought to capture only physiological connectivity. Additional details on the eLORETA connectivity algorithm can be found in Pascual-Marqui et al (15). In the current study, lagged phase synchronization was computed in the theta (4.5-7 Hz) and beta (12.5-21 Hz) frequency bands using a normalized Fourier transform.

Supplementary Results

Models showing significant connectivity effects at only the intercept or the slope, but not both

Two of the connectivity variables under consideration were found to have significant effects at either the intercept or the slope, but not both, specifically:

In the beta band, there was a significant *Connectivity x Time* interaction (effect on the slope) for rACC-PCC (the DMN hub) connectivity (B=-0.54, 95% CI=-1.00, -0.09, $p=0.02$) but the main effect of *Connectivity* (effect at intercept) was at trend (B=-2.12, 95% CI=-4.59, 0.36, $p=0.09$). Exploratory analyses confirmed that adding beta-band rACC-PCC connectivity terms did not provide a significantly better model fit compared to the reduced model that contained the covariates and rACC theta activity (LR=5.62, $p=0.06$).

Also in the beta band, there was a main effect of *Connectivity* (effect at intercept) for rACC-rAI (the SN hub) connectivity (B=2.75, 95% CI=0.15, 5.35, $p=0.04$) however the *Connectivity x Time* interaction term was not significant (B=0.10, 95% CI=-0.38, 0.58, $p=0.68$). The addition of beta-band rACC-rAI connectivity terms did not provide a better model fit than the reduced model containing covariates and rACC theta activity model (LR=5.20, $p=0.07$).

Results of mediation models

For illustration purposes, the results of the two mediation models tested are shown in Figure S2. The indirect effect of baseline rACC theta activity on HRSD improvement through baseline theta-band rACC-rAI connectivity was -0.17 (SE=0.30; 95% CI=-0.88, 0.34). In the second mediation model, where change in theta-band rACC-rAI connectivity from baseline to week 1 was evaluated as the potential mediator, the indirect effect was 0.02 (SE=0.03; 95% CI= -0.49, 0.49). The inclusion of

zero within the CIs for both models indicated that neither baseline theta-band rACC-rAI connectivity nor early change (baseline to week 1) in this connectivity was a mediator.

Control analyses examining potential confounds in the link between theta-band rACC-rAI connectivity and remission status

The between-subjects variability in theta-band rACC-rAI connectivity at baseline and week 1, between the placebo and sertraline groups is shown in Fig. S3. As is evident, there were no differences in connectivity between the groups at either time point.

Theta-band rACC-rAI connectivity changes from baseline to week 1 predicted remission status after controlling for baseline HRSD scores (odds ratio=2.90, 95% CI=1.11, 7.58, $p=0.03$). Aligning with the absence of moderation or mediation effects, we confirmed that theta-band rACC-rAI connectivity changes predicted remission status even when rACC theta activity change was entered into the model (odds ratio=2.94, 95% CI=1.12, 7.71, $p=0.03$) indicating that the relationship between early theta-band rACC-rAI connectivity changes and symptom remission was not related to early rACC theta activity changes. Theta-band rACC-rAI connectivity also remained a significant predictor when recruitment site was entered into the model as a covariate ($p=0.04$).

Link between rACC connectivity and depression chronicity

Relative to those with non-chronic MDD at baseline ($n=122$), those with chronic (episode duration longer than 2 years) MDD ($n=116$) had lower baseline theta-band rACC-rAI connectivity, $t(236)=2.83$, $p=0.005$, Cohen's $d=0.37$ [chronic $M=-1.12$, $SD=0.22$; non-chronic $M=-1.04$, $SD=0.21$]. This was not driven by differences in symptom severity, as chronic and non-chronic MDD patients did not differ in baseline HRSD scores, $t(236)=-0.62$, $p=0.53$, and connectivity differences remained significant when controlling for baseline HRSD scores, $F(1, 235)=7.93$, $p=0.005$, $\eta_p^2=0.03$.

Tests of whether early changes in theta-band rACC-rAI connectivity reflect a marker of depression remission that is already in progress during the first week of treatment

As requested by an anonymous Reviewer, we examined whether remitters who were predicted by early changes in theta-band rACC-rAI connectivity were those who showed a decline in HRSD scores from baseline to week 1. If this were the case, then this may indicate that early changes in theta-band rACC-rAI connectivity represents a potential marker of depression remission that is already in progress during the first week of treatment.

To do this, we generated the predicted group membership (remitter vs. non-remitter) from the binary logistic regression model examining the degree to which early changes in theta-band rACC-rAI connectivity from baseline to week 1 predict depression remission status at week 8. The model accurately classified 109 of the 122 individuals who did not remit (89.3% accuracy) but only 12 of the 73 individuals who did remit (16.4% accuracy). Next, we ran a *Remitter* (predicted remitter, predicted non-remitter) x *Week* (baseline, week 1) repeated measures ANOVA to determine whether predicted remitters showed greater depressive symptom reductions from baseline to week 1 relative to predicted non-remitters. Of the 195 individuals with remission status data available, 186 had HRSD data at both baseline and week 1. The *Remitter* x *Week* interaction was not significant, $F(1,184)=0.09$, $p=0.73$, $\eta_p^2<0.001$, indicating that the predicted remitters and predicted non-remitters did not differ in their overall change in HRSD scores from baseline to week 1. There was a main effect of *Week*, $F(1,184)=25.06$, $p<0.001$, $\eta_p^2=0.12$, where across both groups, HRSD scores decreased significantly from baseline to week 1. Furthermore, there was a main effect of *Remitter*, $F(1,184)=23.75$, $p<0.001$, $\eta_p^2=0.11$, where averaged across baseline and week 1, the HRSD scores of the predicted remitters

was significantly lower than the predicted non-remitters (predicted remitters: $M=13.60$, $SE=0.76$; predicted non-remitters: $M=17.58$, $SE=0.29$).

These results suggest that remitters, as predicted by early changes in theta-band rACC-rAI connectivity, were more likely to have lower HRSD scores at the beginning of treatment. This is consistent with the widely-replicated link between lower baseline depression severity and greater responses to treatment.

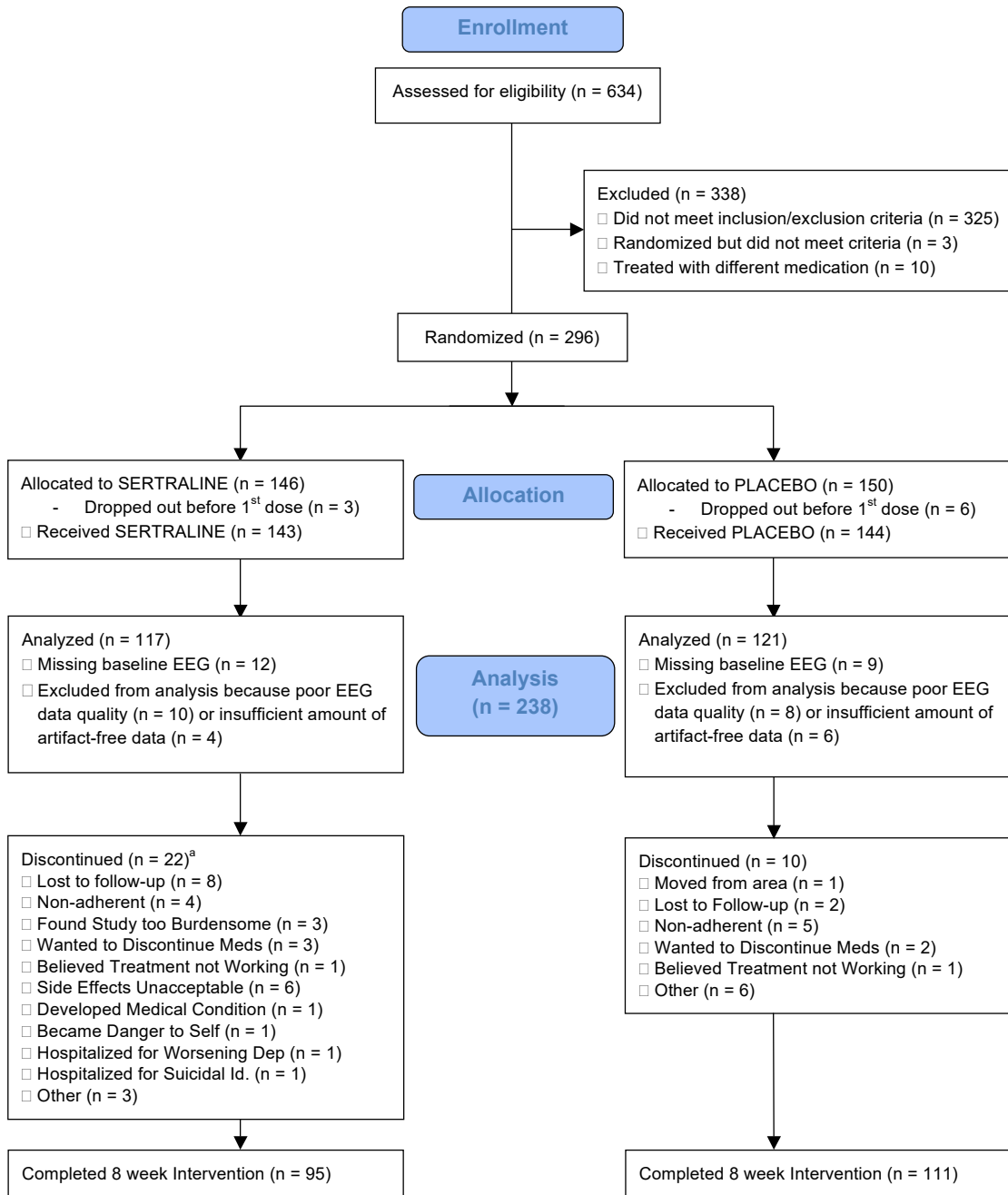
Symptom trajectories in first and second-stage treatment remitters

At the suggestion of an anonymous Reviewer, we also conducted an exploratory analysis that sought to compare the symptom trajectories of individuals who remitted at the first stage of treatment (i.e., at week 8 and who were predicted by early changes in theta-band rACC-rAI connectivity) to individuals who remitted after a second stage of treatment (i.e., at week 16 and who were not predicted by early changes in theta-band rACC-rAI connectivity) to individuals who never remitted.

The second stage of treatment was conducted from weeks 9 to 16, where some individuals who were randomized to placebo at the first stage of treatment received either placebo or sertraline at the second stage, and some individuals who received sertraline at the first stage were randomized to sertraline again, or to bupropion or placebo at the second stage. To inspect the rate of symptom improvement, we first divided the sample into those who remitted at the first stage of treatment (i.e., those who had a HRSD score ≤ 7 at week 8), those who remitted at the second stage of treatment (i.e., those who had a HRSD score ≤ 7 at week 16), and those who never remitted (i.e., those who had a HRSD score > 7 at week 16) and plotted the raw mean HRSD (\pm SEM) scores over time (Fig. S4). Pairwise comparisons focused on differences in HRSD scores at week 8, since early changes in theta-band rACC-rAI connectivity predicted remission status at week 8.

Results showed that week 8 HRSD scores in second stage remitters ($M=12.87$, $SD=3.42$) were significantly higher than first stage remitters ($M=3.96$, $SD=2.25$), $t(119)=17.27$, $p<0.001$, but were

significantly lower than non-remitters ($M=16.65$, $SD=5.25$), $t(129)=18.84$, $p<0.001$. These findings suggest that second stage remitters fall intermediate between remitters who were predicted by early changes in theta-band rACC-rAI connectivity (i.e., first-stage remitters) and non-remitters in terms of symptom severity. It is possible that second stage remitters may be captured by changes in theta-band rACC-rAI connectivity over a longer time course (e.g., from baseline to week 8). Although EEG data were only obtained at baseline and week 1 in the current study, future studies examining changes in theta-band rACC-rAI connectivity over a longer time course would assist in determining whether this connectivity marker reflects remission that is “in progress” or whether it is a marker that indicates a person’s likelihood of achieving remission/early response.



^aNote that there are more reasons for exclusion than there are total discontinued participants as some participants discontinued for more than one reason.

Figure S1. CONSORT flow diagram showing numbers of participants who were randomized to treatment, who received treatment, who had valid EEG data available for the current analyses, and who completed 8 weeks of treatment.

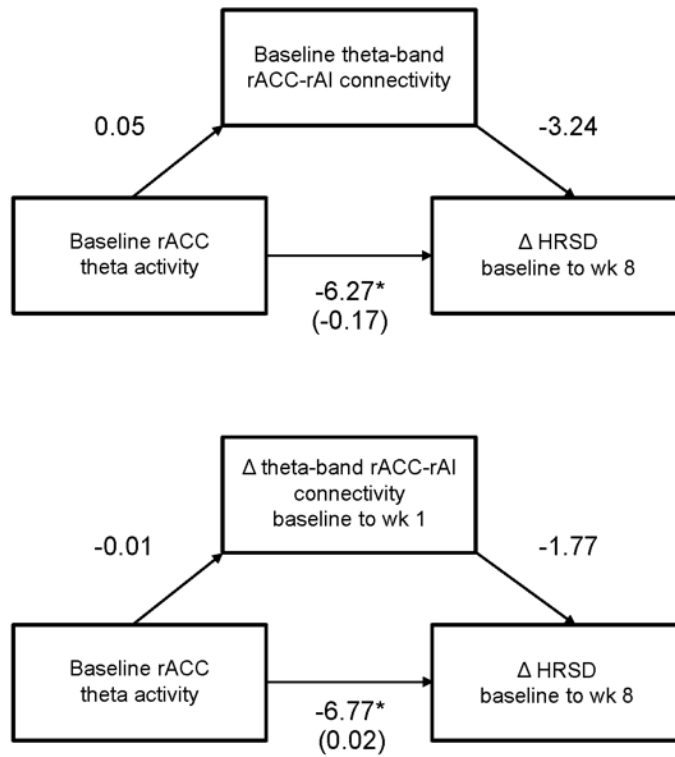


Figure S2. Figure shows mediation models examining the indirect (mediating) effect of baseline theta-band rACC-rAI connectivity (top model) and changes in theta-band rACC-rAI connectivity from baseline to week 1 (bottom model) as potential mediators of the link between elevated baseline rACC theta activity and greater reduction in HRSD scores from baseline to week 8. Neither model shows evidence of theta-band rACC-rAI connectivity acting as a mediator. rACC=rostral anterior cingulate cortex; rAI=right anterior insula, ΔHRSD=change in Hamilton Rating Scale for Depression scores from baseline to week 8; *=significant at $p < 0.05$.

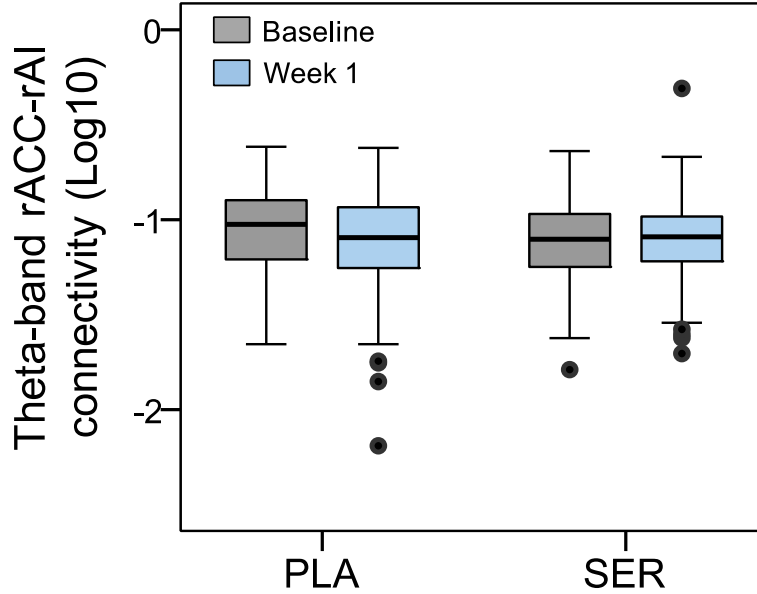


Figure S3. Box plots showing the between-subject variability in theta-band rACC-rAI connectivity between the placebo (PLA) and sertraline (SER) groups at baseline (grey bars) and week 1 (blue bars). Cases represented by black dots are greater than $\pm 2SD$ from the mean but less than $\pm 3SD$, and are not considered outliers. The figure shows that there were no differences in theta-band rACC-rAI connectivity between the two treatment arms either at baseline or at week 1. This suggests that early changes in theta-band rACC-rAI connectivity and their relationship with depression remission at week 8 cannot be solely attributable to the acute effects of sertraline (since the same effects were observed for the placebo group). This further highlights theta-band rACC-rAI connectivity as a prognostic, yet treatment non-specific indicator of depression improvement.

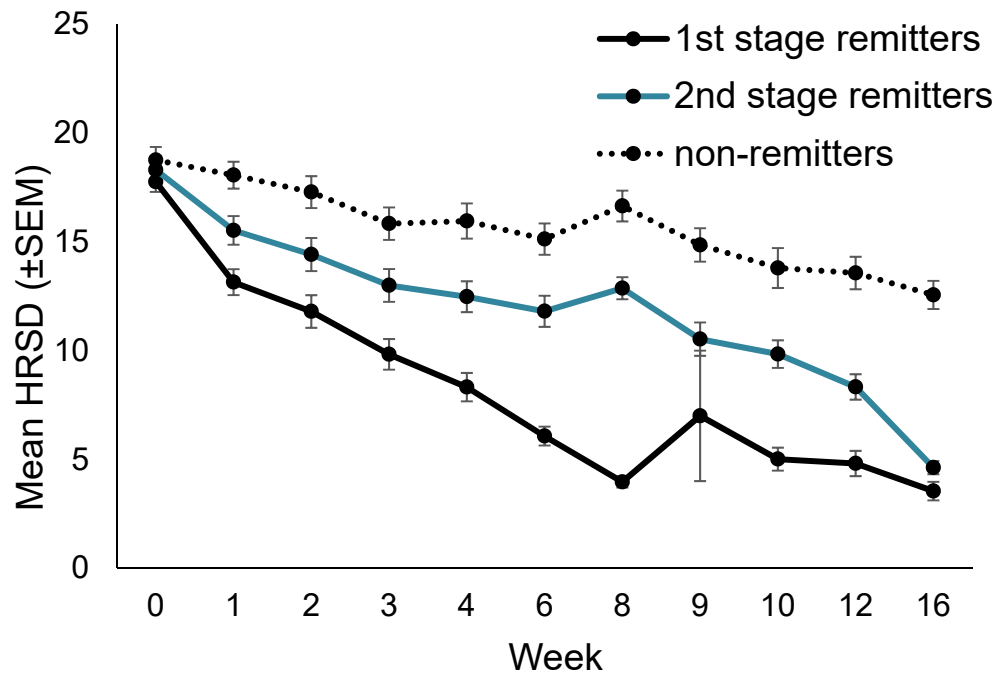


Figure S4. Mean (\pm SEM) HRSD scores across the first stage (weeks 0-8) and second stage (weeks 9-16) of treatment in individuals who were classified as: 1st stage remitters (HRSD \leq 7 by week 8); 2nd stage remitters (HRSD \leq 7 by week 16); non-remitters (HRSD $>$ 7 at weeks 8 and 16).

Table S1. Reasons for participant dropout across the sertraline and placebo groups

Discontinued Sertraline (n=26)	Discontinued Placebo (n=19)
Lost to follow-up (n=7)	Lost to follow-up (n=5)
Non-adherent (n=6)	Non-adherent (n=6)
Wanted to discontinue medication (n=3)	Wanted to discontinue medication (n=4)
Believed treatment was not working (n=1)	Believed treatment was not working (n=2)
Side effects unacceptable (n=9)	Side effects unacceptable (n=1)
Found study too burdensome (n=3)	Moved from area (n=1)
Developed medical condition (n=1)	Became pregnant (n=1)
Became danger to self (n=1)	Other (n=6)
Hospitalized for worsening depression (n=1)	
Hospitalized for suicidal ideation (n=1)	
Other (n=4)	

Note. Numbers add up to more than the totals because participants discontinued for more than one reason.

Table S2. Seed regions used for connectivity analyses

Region	X	Y	Z	Reference
Rostral anterior cingulate cortex	11	45	-6	Pizzagalli et al. (2001), Fig. 1
Posterior cingulate cortex	0	-52	26	Yeo et al. (2011), Table 5
Left dorsolateral prefrontal cortex	-43	22	34	Dosenbach et al. (2007), Table 1
Right anterior insula	42	10	-12	Seeley et al. (2007) Supp. Table 2

Note. X=left(-) to right(+); Y=posterior(-) to anterior(+); Z=inferior(-) to superior(+). Note that regions-of-interest were not registered to subject space from the MNI template, but rather, were retained in MNI space.

Table S3. Demographic and clinical factors that have been identified as predictors of poor outcome in prior studies of depression. Variables capturing each of these factors were used as covariates in our final model and the model reported in Table 2 of Pizzagalli, Webb, et al. (2018)

Covariate	Reference
Greater baseline depression severity (QIDS-SR, HRSD)	Trivedi <i>et al.</i> (2006)
Anxious depression (anxiety factor score on the HRSD)	Fava <i>et al.</i> (2008)
Anhedonia (CIDI)	Spijker <i>et al.</i> (2001)
Male gender	Trivedi <i>et al.</i> (2006)
Older age	Fournier <i>et al.</i> (2009)
Lower socioeconomic status	Jakubovski <i>et al.</i> (2014)
Being non-Caucasian	Trivedi <i>et al.</i> (2006)
Being unmarried	Fournier <i>et al.</i> (2009)

Note. QIDS-SR=Quick Inventory of Depressive Symptoms, Self-Report; HRSD=Hamilton Rating Scale for Depression; CIDI=Composite International Diagnostic Interview.

Table S4. Demographic and clinical characteristics of the sertraline and placebo groups for the subsample included in the current analysis (n=238)

	Whole sample (n=238)	Sertraline (n=117)	Placebo (n=121)	<i>P</i> Value
Age in years, M (SD)	36.9 (13.2)	36.6 (13.5)	37.3 (13.0)	0.68
Female, No. (%)	151 (63.4)	79 (67.5)	72 (59.5)	0.20
Years of education, M (SD)	15.1 (2.4)	14.9 (2.4)	15.3 (2.4)	0.21
Caucasian, No. (%)	163 (68.5)	78 (66.7)	85 (70.2)	0.55
Hispanic, No. (%)	42 (17.6)	20 (17.1)	21 (17.4)	0.90
Married, No. (%)	49 (20.6)	22 (26.5)	29 (24.0)	0.19
Employed, No. (%)	135 (56.7)	64 (54.7)	71 (58.7)	0.54
Age of MDD onset, M (SD)	16.3 (5.7)	16.5 (5.8)	16.1 (5.6)	0.63
Current MDE length (months), median	15.5	13.0	18.0	0.49
Number of prior MDEs, median	4	4	5	0.42
QIDS, M (SD)	18.2 (2.8)	18.6 (2.8)	17.7 (2.8)	0.02
HRSD 17-item, M (SD)	18.5 (4.5)	18.4 (4.5)	18.5 (4.4)	0.89

Note. MDD=Major Depressive Disorder; MDE=Major Depressive Episode; QIDS=Quick Inventory of Depressive Symptoms; HRSD=Hamilton Rating Scale for Depression; *P* Values indicate the significance value for tests of differences between the sertraline and placebo group.

Supplementary References

1. Tenke CE, Kayser J, Pechtel P, Webb CA, Dillon DG, Goer F, *et al.* (2017): Demonstrating test-retest reliability of electrophysiological measures for healthy adults in a multisite study of biomarkers of antidepressant treatment response. *Psychophysiology* 54: 34-50.
2. Perrin F, Pernier J, Bertrand O, Echallier J. (1989): Spherical splines for scalp potential and current density mapping. *Electroencephalogr Clin Neurophysiol* 72: 184-187.
3. NeuroScan I. (2003): SCAN 4.3 - Vol. II. EDIT 4.3 - Offline analysis of acquired data (Document number 2203, Revision D). Compumedics Neuroscan, El Paso, TX.
4. Kayser J, Tenke CE. (2006): Electrical distance as a reference-free measure for identifying artifacts in multichannel electroencephalogram (EEG) recordings. *Psychophysiology* 43: S51.
5. Mobascher A, Brinkmeyer J, Warbrick T, Musso F, Wittsack HJ, Stoermer R, *et al.* (2009): Fluctuations in electrodermal activity reveal variations in single trial brain responses to painful laser stimuli — A fMRI/EEG study. *Neuroimage* 44: 1081-1092.
6. Rullmann M, Anwander A, Dannhauer M, Warfield SK, Duffy FH, Wolters CH. (2009): EEG source analysis of epileptiform activity using a 1 mm anisotropic hexahedra finite element head model. *Neuroimage* 44: 399-410.
7. Worrell GA, Lagerlund TD, Sharbrough FW, Brinkmann BH, Busacker NE, Cicora KM, *et al.* (2000): Localization of the epileptic focus by low-resolution electromagnetic tomography in patients with a lesion demonstrated by MRI. *Brain Topogr* 12: 273-282.
8. Vitacco D, Brandeis D, Pascual-Marqui R, Martin E. (2002): Correspondence of event-related potential tomography and functional magnetic resonance imaging during language processing. *Hum Brain Mapp* 17: 4-12.
9. Mulert C, Jäger L, Schmitt R, Bussfeld P, Pogarell O, Möller H-J, *et al.* (2004): Integration of fMRI and simultaneous EEG: towards a comprehensive understanding of localization and time-course of brain activity in target detection. *Neuroimage* 22: 83-94.
10. Dierks T, Jelic V, Pascual-Marqui RD, Wahlund L-O, Julin P, Linden DE, *et al.* (2000): Spatial pattern of cerebral glucose metabolism (PET) correlates with localization of intracerebral EEG-generators in Alzheimer's disease. *Clin Neurophysiol* 111: 1817-1824.
11. Pizzagalli D, Oakes T, Fox A, Chung M, Larson C, Abercrombie H, *et al.* (2004): Functional but not structural subgenual prefrontal cortex abnormalities in melancholia. *Mol Psychiatry* 9: 393-405.
12. Zumsteg D, Wennberg R, Treyer V, Buck A, Wieser H. (2005): H215O or 13NH3 PET and electromagnetic tomography (LORETA) during partial status epilepticus. *Neurology* 65: 1657-1660.
13. Grech R, Cassar T, Muscat J, Camilleri KP, Fabri SG, Zervakis M, *et al.* (2008): Review on solving the inverse problem in EEG source analysis. *J Neuroeng Rehabil* 5: 25-58.

14. Pascual-Marqui RD, Faber PL, Kinoshita T, Kochi K, Milz P, Nishida K, *et al.* (2018): Comparing EEG/MEG neuroimaging methods based on localization error, false positive activity, and false positive connectivity. *bioRxiv*: 269753.
15. Pascual-Marqui RD, Lehmann D, Koukkou M, Kochi K, Anderer P, Saletu B, *et al.* (2011): Assessing interactions in the brain with exact low-resolution electromagnetic tomography. *Philos Trans A Math Phys Eng Sci* 369: 3768-3784.
16. Pizzagalli DA, Pascual-Marqui RD, Nitschke JB, Oakes TR, Larson CL, Abercrombie HC, *et al.* (2001): Anterior cingulate activity as a predictor of degree of treatment response in major depression: evidence from brain electrical tomography analysis. *Am J Psychiatry* 158: 405-415.
17. Yeo BT, Krienen FM, Sepulcre J, Sabuncu MR, Lashkari D, Hollinshead M, *et al.* (2011): The organization of the human cerebral cortex estimated by intrinsic functional connectivity. *J Neurophysiol* 106: 1125-1165.
18. Dosenbach NU, Fair DA, Miezin FM, Cohen AL, Wenger KK, Dosenbach RA, *et al.* (2007): Distinct brain networks for adaptive and stable task control in humans. *Proc Natl Acad Sci USA* 104: 11073-11078.
19. Seeley WW, Menon V, Schatzberg AF, Keller J, Glover GH, Kenna H, *et al.* (2007): Dissociable intrinsic connectivity networks for salience processing and executive control. *J Neurosci* 27: 2349-2356.
20. Trivedi MH, Rush AJ, Wisniewski SR, Nierenberg AA, Warden D, Ritz L, *et al.* (2006): Evaluation of outcomes with citalopram for depression using measurement-based care in STAR*D: implications for clinical practice. *Am J Psychiatry* 163: 28-40.
21. Fava M, Rush AJ, Alpert JE, Balasubramani G, Wisniewski SR, Carmin CN, *et al.* (2008): Difference in treatment outcome in outpatients with anxious versus nonanxious depression: a STAR* D report. *Am J Psychiatry* 165: 342-351.
22. Spijker J, Bijl R, De Graaf R, Nolen W. (2001): Determinants of poor 1-year outcome of DSM-III-R major depression in the general population: results of the Netherlands Mental Health Survey and Incidence Study (NEMESIS). *Acta Psychiatr Scand* 103: 122-130.
23. Fournier JC, DeRubeis RJ, Shelton RC, Hollon SD, Amsterdam JD, Gallop R. (2009): Prediction of response to medication and cognitive therapy in the treatment of moderate to severe depression. *J Consult Clin Psychol* 77: 775-787.
24. Jakubovski E, Bloch MH. (2014): Prognostic subgroups for citalopram response in the STAR*D trial. *J Clin Psychiatry* 75: 738-747.